



Palladium(II) and platinum(II) complexes with *N*1-hydroxyethyl-3,5-pyrazole derived ligands

José A. Perez^a, Vanessa Montoya^a, José A. Ayllon^a, Mercè Font-Bardia^{b,c}, Teresa Calvet^{b,c}, Josefina Pons^{a,*}

^a Departament de Química, Universitat Autònoma de Barcelona, Bellaterra, 08193 Barcelona, Spain

^b Cristallografia, Mineralogia i Dipòsits Minerals, Universitat de Barcelona, Martí i Franquès s/n, 08028 Barcelona, Spain

^c Unitat de Difracció de RX, Centres Científics i Tecnològics de la Universitat de Barcelona, Solé i Sabaris 1-3, 08028, Barcelona, Spain

ARTICLE INFO

Article history:

Received 23 March 2012

Received in revised form 2 July 2012

Accepted 26 July 2012

Available online 11 August 2012

Keywords:

N-Hydroxyalkylphenylpyrazole

Regioisomers

Palladium(II)

Platinum(II)

Crystal structures

ABSTRACT

Reaction of the ligands 2-(5-methyl-3-phenyl-1*H*-pyrazol-1-yl)ethanol (**L1**) and 2-(3-methyl-5-phenyl-1*H*-pyrazol-1-yl)ethanol (**L2**) with $[\text{MCl}_2(\text{CH}_3\text{CN})_2]$ ($\text{M} = \text{Pd}(\text{II}), \text{Pt}(\text{II})$) gave the complexes *trans*- $[\text{MCl}_2\text{L}_2]$ ($\text{M} = \text{Pd}(\text{II})$ and $\text{Pt}(\text{II})$, $\text{L} = \text{L1}, \text{L2}$).

The new complexes were characterised by elemental analyses, conductivity measurements, mass spectrometry, IR, ¹H and ¹³C{¹H} NMR spectroscopies. The crystal and molecular structures of the ligand **L2** and the complexes *trans*- $[\text{PdCl}_2\text{L}_2]$ ($\text{L} = \text{L1}, \text{L2}$) were resolved by X-ray diffraction. Both palladium complexes consisted on monomeric *trans*- $[\text{PdCl}_2\text{L}_2]$ ($\text{L} = \text{L1}, \text{L2}$) species and molecular packing is determined by intermolecular hydrogen bonding interactions.

The NMR spectra of the complexes $[\text{PdCl}_2\text{L}_2]$ ($\text{L} = \text{L1}, \text{L2}$) in CDCl₃ solution, is consistent with a very slow rotation of the pyrazolic ligands around the Pd–N bond, so that two conformational isomers can be observed in solution (*syn* and *anti*). Different behaviour was observed for complexes $[\text{PtCl}_2\text{L}_2]$ ($\text{L} = \text{L1}, \text{L2}$), for which only the *anti* isomer was detected in CDCl₃ solution at room temperature.

© 2012 Elsevier B.V. All rights reserved.

1. Introduction

Coordination chemistry of palladium(II) and platinum(II) complexes with heterocyclic ligands with two potential donor atoms is one of the research areas that has undergone a fast development during the last years [1]. Among all the examples reported so far, those containing pyrazole derivatives are especially attractive because they have multiple applications. For example, similar complexes (pyridylpyrazole ligands with Pt(II)) have shown greater antitumor activity and lower toxicity than the common *cis*- $[\text{PtCl}_2(\text{NH}_3)_2]$ complex [2]. Applications of palladium and platinum complexes including pyrazolic ligands extend also to macromolecular chemistry [3] and homogeneous catalysis [4].

Properties of the pyrazole ligand can be modified through substitution of the protons, yielding a great diversity of pyrazolyl derivatives. The nature of the substituents, size and functionalization, determines the chemical and structural characteristics of metal complexes formed with these pyrazole derivative ligands.

We have previously studied 1,3,5-substituted pyrazole derived ligands, including only substituents without donor atoms (alkyl, phenyl), or with donor atoms with low coordination power (ether,

polyether, tioether). These pyrazole derivative ligands coordinate to palladium and platinum only through the azine nitrogen, acting thus as monodentate ligand. This is the case of the complexes with stoichiometry $[\text{MCl}_2(\text{N}_{\text{pz}})_2]$ ($\text{M} = \text{Pd}(\text{II})$ or $\text{Pt}(\text{II})$, $\text{pz} = 1,3,5$ -substituted pyrazole ligand). In these complexes, it can exist two different isomers: *cis* or *trans* which are defined as a function on the arrangement of the chlorine or pyrazolyl ligands [5]. For all the palladium complexes the *trans* isomer was obtained, as it minimizes the steric hindrance between the two pyrazolyl ligands, also the NMR studies in solution have proved the existence of conformational diastereoisomers, *anti* and *syn*, defined by the relative disposition of the *N*1 attached group, while all analysed crystal structures correspond to the *anti* isomer, suggesting that this isomer is the most stable one in solid state. In the case of platinum complexes, *cis* and *trans* isomers have been found in the solid state [5b–d]. This difference in the disposition of the chlorine atoms between Pd(II) and Pt(II) complexes with similar ligands had already been observed in the literature [6,7], and generally, it is explained by the considerable higher lability of ligand–Pd(II) bonds compared to ligand–Pt(II).

In particular, in this work we have reported the synthesis and structural characterisation of new palladium(II) and platinum(II) complexes with *N*1-hydroxyethyl-3,5-substituted pyrazole ligands. Moreover, in order to see whether the hindered rotation around the metal–N bond in solution is caused by the bulk substituents in 3,5-disposition, by the lengths of the *N*1-substituents or

* Corresponding author. Address: Departament de Química, Facultat de Ciències, Universitat Autònoma de Barcelona, Bellaterra-Cerdanyola, 08193 Barcelona, Spain. Fax: +34 93 581 31 01.

E-mail address: Josefina.Pons@uab.es (J. Pons).

by the nature of the metal, the related Pd(II) and Pt(II) isomer formation with these ligands have been investigated by NMR and compared with previous results obtained with similar complexes.

2. Results and discussion

2.1. Synthesis and general characteristics of the ligands

1-Phenyl-1,3-butanedione [8] was the precursor for the synthesis of the ligands. This β -dione was prepared by Claisen condensation of ethyl acetate and acetophenone using sodium ethoxide (NaOEt) as base and dry toluene as solvent [9]. Treatment of this β -dione with 2-hydroxyethylhydrazine in absolute ethanol at room temperature during 16 h produced two regioisomers, 2-(5-methyl-3-phenyl-1*H*-pyrazol-1-yl)ethanol (**L1**) and 2-(3-methyl-5-phenyl-1*H*-pyrazol-1-yl)ethanol (**L2**) in a 98% yield (Scheme 1). The higher reaction time required for this synthesis compared with similar ones described in the literature is probably due to both electronic and steric hindrance effects of the methyl group [10]. The separation of the two regioisomers was carried out by silica column chromatography using ethyl acetate as eluent. A 50:50 regioisomer ratio (**L1**:**L2**) was calculated through the integration of the pyrazolic proton signals in the ^1H NMR spectrum. When the same reaction was carried out at low temperature (-84°C), the formation of the kinetic regioisomer (**L2**) was favoured and the regioisomer ratio was 24:76 (**L1**:**L2**).

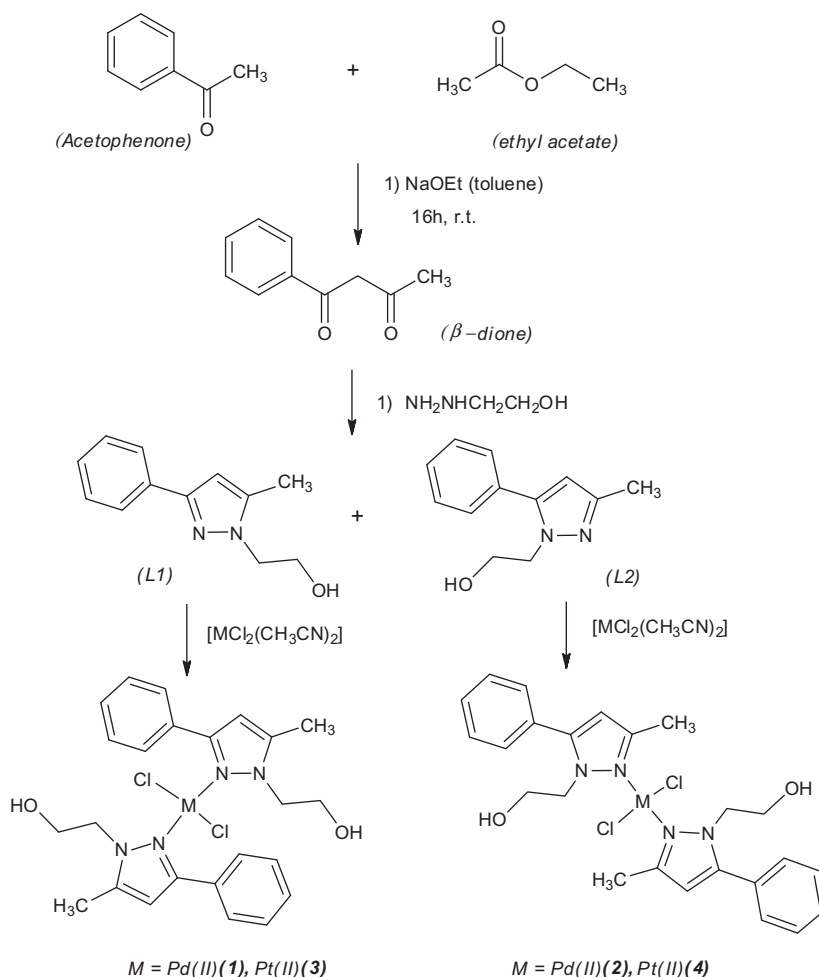
Both regioisomers were characterised by elemental analyses, mass spectrometry, IR, ^1H , $^{13}\text{C}\{^1\text{H}\}$, COSY, HSQC and NOESY NMR

spectroscopy, mass spectrometry. **L2** regioisomer was further characterised by X-ray diffraction. The assignment of each one of the regioisomers was confirmed by NOESY experiments. Regioisomer **L1** presents NOE-interactions between the protons of the hydroxyalkyl chain and the methyl group. For **L2**, NOE-interactions between the protons of hydroxyalkyl chain and the phenyl group are observed.

The more distinctive signals in the ^1H NMR are those assigned to *ortho*-phenyl hydrogen at $\delta = 7.76$ ppm ($^3J = 5.1$ Hz) (**L1**), and $\delta = 7.42$ ppm ($^3J = 4.7$ Hz) (**L2**) as doublets and the assigned to the pyrazolic hydrogen at $\delta = 6.19$ ppm (**L1**) and 5.96 ppm (**L2**). Other signals attributed to the *meta*- and *para*-phenyl hydrogens are present as a multiplete. The $^{13}\text{C}\{^1\text{H}\}$ NMR spectra display the signals at $\delta = 102.4$ ppm (**L1**) and 105.6 ppm (**L2**), attributable to the CH of the pyrazole [11]. In the mass spectrum (ESI(+)-MS) of **L1** and **L2** ligands, one signal is observed at 203 (100%), attributable to $[\text{L}+\text{H}]^+$ ($\text{L} = \text{L1}, \text{L2}$).

The structure of **L2** ligand was confirmed by single crystal X-ray diffraction from prismatic crystals obtained by the slow evaporation of an ethyl acetate solution of a mixture of **L1** and **L2** ligands. The quality of crystal was poor but the X-ray diffraction analysis could be carried out and clearly revealed the structure of the ligand.

ORTEP picture of **L2** with the atom numbering scheme is shown in Fig. 1. The phenyl group is twisted with respect to the pyrazole and the asymmetric unit consists of four molecules that differ in the angles between these rings ($42.7(2)^\circ$, $44.7(2)^\circ$, $38.1(2)^\circ$ and $40.3(2)^\circ$), respectively. Each molecule is linked to other two via



Scheme 1.

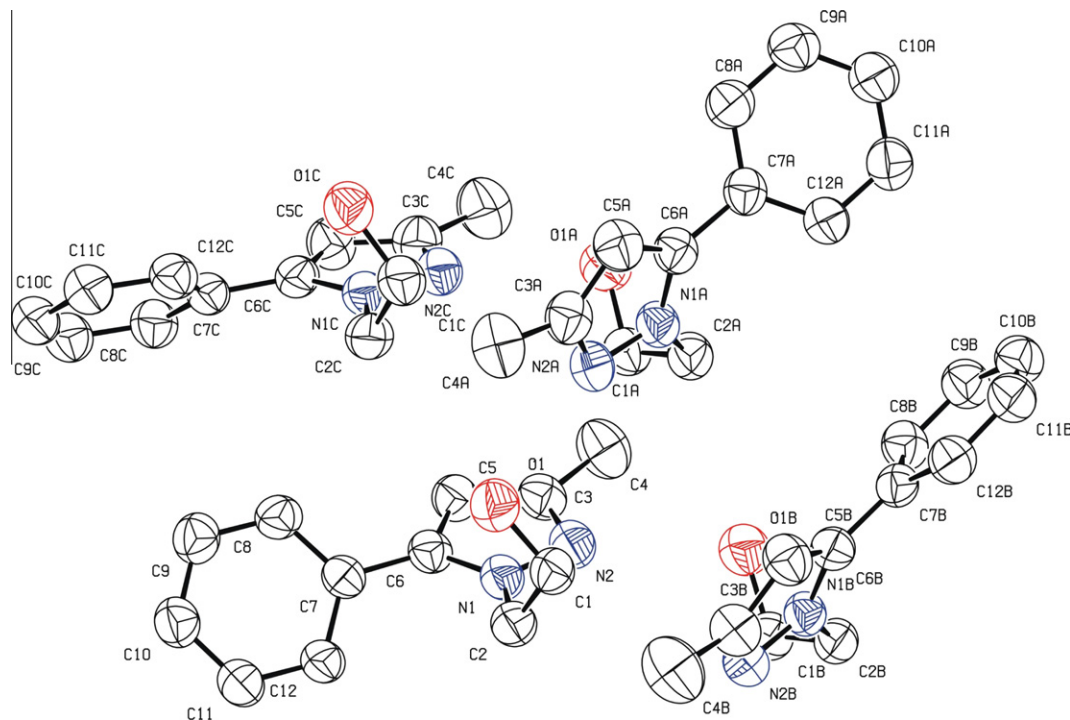


Fig. 1. ORTEP view of the **L2** asymmetric unit with atom labelling scheme. Thermal ellipsoids were drawn at 50% probability. Hydrogen atoms are omitted for clarity.

hydrogen bonds between the proton of the alcohol ($\text{CH}_2\text{-CH}_2\text{-OH}$) and the free pair electrons of the pyrazolic nitrogen ($\text{O-H}\cdots\text{N}$). The $\text{O-H}\cdots\text{N}$ distances and the angles showed in Table 1 are in agreement with other values described in the literature [6,12]. These

Table 1
Distances (Å) and angles ($^\circ$) of hydrogen bonds of **L2**.

O-H \cdots N	O-H (Å)	O-H \cdots N (Å)	O \cdots N (Å)	O-H \cdots N ($^\circ$)
O(1)-H(1) \cdots N(2A) ⁱ	0.82	2.18	2.924(4)	151
O(1A)-H(1A1) \cdots N(2C) ⁱ	0.82	2.13	2.850(4)	146
O(1C)-H(1C) \cdots N(2B) ⁱ	0.82	2.13	2.801(4)	140
O(1)-H(1B1) \cdots N(2) ⁱⁱ	0.82	2.16	2.853(4)	143

Symmetry code: (i) $1-x, 1-y, 1-z$; (ii) $-x, 1-y, 1-z$.

interactions give as a result a supramolecular structure in a zig-zag infinite chains extending in the *a*-axis direction (Fig. 2).

The pyrazole rings of the adjacent molecules are approximately parallel ($14.5(2)^\circ$ and $15.7(2)^\circ$), whereas the phenyl rings are almost perpendicular ($82.8(2)^\circ$ and $81.8(2)^\circ$) in such way that the supramolecular structure is also stabilized by $\text{C-H}\cdots\pi$ interactions involving the phenyl rings. The $\text{C-H}\cdots\text{Cg}$ contact distances between the H atoms of a phenyl groups and the centroid of the neighbouring phenyl rings are: C(9B)-H(9B) \cdots Cg(4) 2.87 Å, symmetry code $-x, 1-y, 1-z$; C(11C)-H(11C) \cdots Cg(2) 2.89 Å, symmetry code $1-x, 2-y, -z$; C(12A)-H(12A) \cdots Cg(6) 2.94 Å, symmetry code $1+x, y, z$; Cg(4), Cg(2) and Cg(6) are the centroids of the phenyl rings numbered C(7A)-C(12A), C(7)-C(12) and C(7B)-C(12B), respectively.

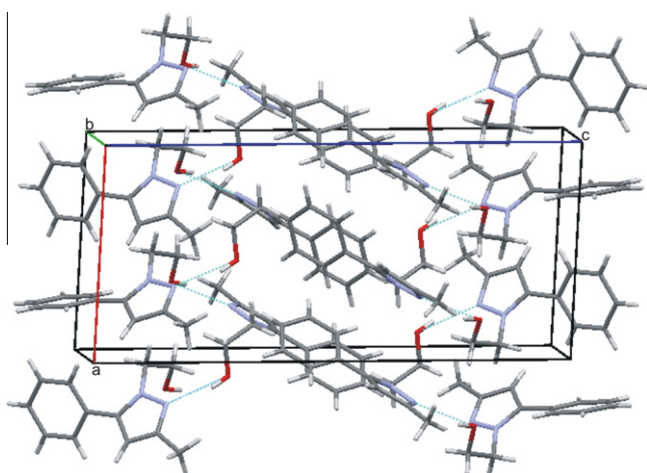


Fig. 2. View of the infinite 3D-structure formed by the different units of **L2** bonded by hydrogen bonds.

2.2. Synthesis and general characterisation of complexes

The reaction of the ligands (**L1**, **L2**) with $[\text{MCl}_2(\text{CH}_3\text{CN})_2]$ ($\text{M} = \text{Pd(II)}$ [13] or Pt(II) [14] in acetonitrile, yielded $[\text{MCl}_2(\text{L1})_2]$ ($\text{M} = \text{Pd(II)}$ (**1**), Pt(II) (**3**)) and $[\text{MCl}_2(\text{L2})_2]$ ($\text{M} = \text{Pd(II)}$ (**2**), Pt(II) (**4**)) complexes. Reactions were performed with 1M:1L or 1M:2L molar ratios and the same results were obtained. Compounds **1-4** were characterised by elemental analyses, mass spectrometry, conductivity measurements, IR and 1D and 2D NMR spectroscopies. The NMR signals were assigned by reference to the literature [11] and from DEPT, COSY, HSQC and NOESY spectra. Single crystal X-ray diffraction was also obtained for the palladium compounds, **1** and **2**. For all complexes, the elemental analyses agreed with the formula $[\text{MCl}_2\text{L}_2]$ ($\text{M} = \text{Pd(II)}$, Pt(II) ; $\text{L} = \text{L1}$, **L2**). The positive ionisation spectra (ESI(+)-MS), of complexes **1-4** showed peaks with *m/z* values of 546 (100%), for **1** and **2**, attributable to $[\text{PdClL}_2]^+$ ($\text{L} = \text{L1}$, **L2**) and 635 (100%) for **3** and **4**, attributable to $[\text{PtClL}_2]^+$ ($\text{L} = \text{L1}$, **L2**). The observed molecular peaks of the cations exhibit the same isotope distribution as predicted theoretically. Conductivity values of 10^{-3} M samples in methanol, for all

compounds, were in agreement with the presence of non-electrolyte compounds [15].

IR spectra of complexes **1–4** in KBr pellets display absorptions of the *N*-hydroxyalkylmethylphenylpyrazole ligands. For all complexes, the most characteristic bands are those attributable to the pyrazole and phenyl groups: [$\nu(\text{C}=\text{C})$, $\nu(\text{C}=\text{N})$] ($1559\text{--}1554\text{ cm}^{-1}$), [$\delta(\text{C}=\text{C})$, $\delta(\text{C}=\text{N})$] ($1500\text{--}1437\text{ cm}^{-1}$), $\delta(\text{C}-\text{H})_{\text{oop}}$ ($812\text{--}768\text{ cm}^{-1}$). It is worth noting that, in the IR spectra of the four compounds, a typical broad band appeared between 3448 and 3309 cm^{-1} showing the presence of the alcohol group $\nu(\text{O}-\text{H})$. The shape and position of this band suggests that hydroxyl group participates in hydrogen bonding interactions [16]. IR spectra of all complexes, between 600 and 200 cm^{-1} , were also recorded. The complexes **1** and **2** showed the $\nu(\text{Pd}-\text{N})$ bands at 487 and 494 cm^{-1} , respectively, and complexes **3** and **4** showed the $\nu(\text{Pt}-\text{N})$ bands at 458 and 462 cm^{-1} , respectively [17]. Moreover, these complexes displayed one band between 355 and 344 cm^{-1} , attributable to $\nu(\text{M}-\text{Cl})$ ($\text{M} = \text{Pd}(\text{II})$, $\text{Pt}(\text{II})$), which are typical of compounds with a *trans* disposition of the chlorine atoms around the metal [17].

The NMR spectra of **1–4** were acquired using CDCl_3 as solvent. ^1H NMR and $^{13}\text{C}\{^1\text{H}\}$ NMR spectra for complexes **1** and **2** showed two set of signals for many protons, suggesting the presence of conformational isomers in solution, in an intensity ratio of approximately $1:0.8$ in the case of **1** and $1:0.4$ in **2**. Our previous work also proved that the two species proposed in these cases are the *anti* and the *syn* isomers, respectively, concerning the position of the two carbon chain [5].

Different characteristics of the palladium complexes determine the proportion of the different isomers in solution. When the *N*-alkyl chain increases its length, the less stable isomer (*syn*) decreases its concentration in solution [5c]. The presence of the *syn* and the *anti* isomers is not due to steric factors caused by the substitution (hydrogen, methyl, phenyl or pyridyl) in positions 3 and 5 of the pyrazolic ring [5] (Fig. 3).

In this work, it seemed that the hindrance rotation around metal–ligand bonds, giving these two isomers in solution, was predominantly controlled by the position of the hydroxyalkyl chain in the pyrazole ring. In both complexes the less stable isomer (*syn*) was present in a minor concentration and this difference was especially important for complex **2**.

The presence of two isomers in solution was not observed in complexes $[\text{PtCl}_2\text{L}_2]$ ($\text{L} = \text{L1}(\mathbf{3})$, $\text{L2}(\mathbf{4})$), which showed a unique set of signals for each type of proton and carbon, corresponding to the *anti* conformational isomer.

The ^1H NMR spectra of complexes **3** and **4**, at variable temperature ($298\text{--}233\text{ K}$) did not show any splitting or broadening of signals, which is in agreement with the presence of only one species in solution. In **3** and **4**, the *anti* nature of the isomers was confirmed by NOESY experiments. The complex **3**, showed NOE-interaction between CH_3 group and $\text{CH}_2\text{--CH}_2\text{--OH}$, and in **4**, we observed NOE-interaction between *ortho*- H_{ph} and $\text{CH}_2\text{--CH}_2\text{--OH}$ chain. In these compounds, the rotation around the $\text{Pt}-\text{N}$ bond seemed not

to be possible due to higher $\text{Pt}-\text{N}$ bond rigidity in comparison with $\text{Pd}-\text{N}$.

With these results it seems that the hindrance to rotation around metal–ligand bonds is predominantly controlled by the metal but the influence of steric factor is not negligible [18]. Other precedents in the literature also show that the reactivity of pyrazolic ligands with $\text{Pt}(\text{II})$ yields different results to those obtained with $\text{Pd}(\text{II})$ [5b,5d,7]. It is well known that $\text{Pd}(\text{II})$ is more reactive than $\text{Pt}(\text{II})$ complexes, for example in the literature it is found that palladium complexes interconvert more readily than platinum analogues [19]. NMR studies of rotational barriers for metal–N complexes have also shown that in $\text{Pt}(\text{II})$ complexes, energy barriers are higher than in $\text{Pd}(\text{II})$ complexes [18]. These experimental observations were supported by ab initio calculations of model complexes containing $\text{Pd}-\text{N}$ and $\text{Pt}-\text{N}$ bonds, which reveal that the nitrogen metal $\pi-\sigma$ interactions is stronger for $\text{Pt}(\text{II})$ complexes, resulting in a higher energy rotation barrier [20]. Despite the fact that pyrazole ligands are poor- π -acceptors [21], the experimental finding suggests that the π -effects can be significant in the control of the preferential formation of the rotational diastereoisomers.

Other observed bands are those attributable to H_{pz} , which appear between 6.33 and 6.03 ppm . These values show a displacement compared to the same signal for the free ligands (6.19 ppm (**L1**), 5.96 ppm (**L2**)). The bands attributable to ethylene protons of the $\text{N}_{\text{pz}}\text{--CH}_2\text{--CH}_2\text{--OH}$ chains appear as two triplets between 5.41 and 4.75 ppm and 4.31 and 3.88 ppm , with $^1\text{H}-^1\text{H}$ coupling constants between 6.6 and 5.7 Hz .

In complexes **3** and **4**, the signal attributable to the proton of the alcohol group (OH) is not observed. However in complexes **1** and **2**, this signal appears as a broad band between 3.14 and 2.84 ppm (**1**) and 2.64 and 2.62 ppm (**2**).

Additional $^{195}\text{Pt}\{^1\text{H}\}$ NMR experiments for complexes **3** and **4** at 298 K , presents only one band for each complex. For these complexes, the signals appeared at -2189 and -2152 ppm , respectively. These values are in the range described in the literature for complexes with $[\text{PtCl}_2\text{N}_2]$ core (-2279 , -1198 ppm) [5e,7b,22].

2.3. Crystal and molecular structures for compounds *trans*- $[\text{PdCl}_2(\text{L1})_2](\mathbf{1})$ and *trans*- $[\text{PdCl}_2(\text{L2})_2](\mathbf{2})$

The structures of **1** and **2** were determined by single crystal X-ray diffraction.

ORTEP pictures and selected bond lengths (\AA) and bond angles ($^\circ$) are shown in Figs. 4 and 5 and Table 2. Slow evaporation of chloroform solution of **1** or **2** yielded prismatic orange crystals. The quality of the crystals of complex **2** was not optimal. Other attempts of crystallisation were done, but no single crystals of better quality were obtained. Despite this limitation and the molecular disorder of hydroxyethyl group, the structural refinement proceeded reasonably well, all parameters converging satisfactorily and no abnormal residual electron density being evident.

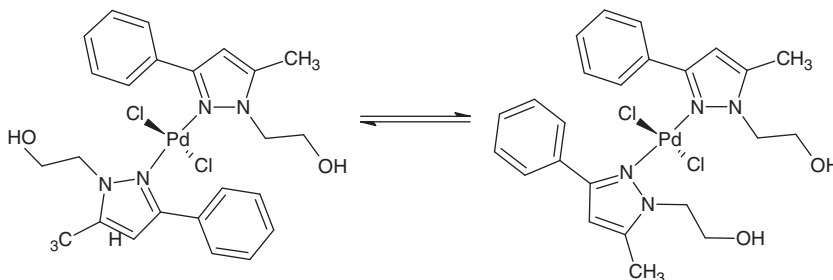


Fig. 3. The conformational isomers existing in solution due to hindered rotation around the $\text{Pd}-\text{N}$ bond at room temperature for compounds **1** and **2**.

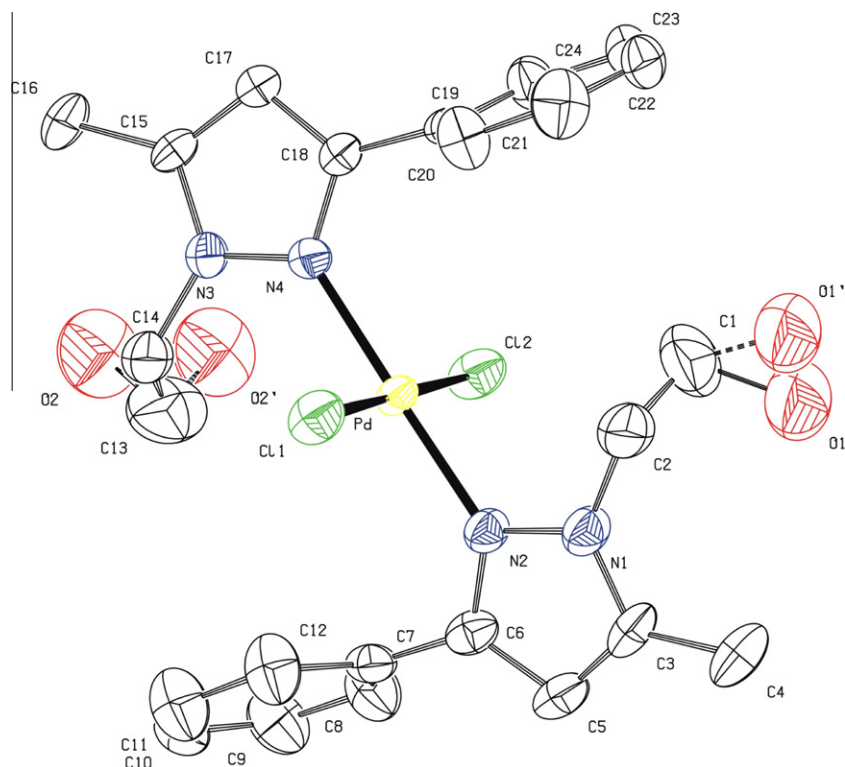


Fig. 4. ORTEP diagram of complex $[\text{PdCl}_2(\text{L1})_2]$ (**1**) showing the atom labelling scheme. 50% Amplitude displacement ellipsoids are shown. Hydrogen atoms are omitted for clarity.

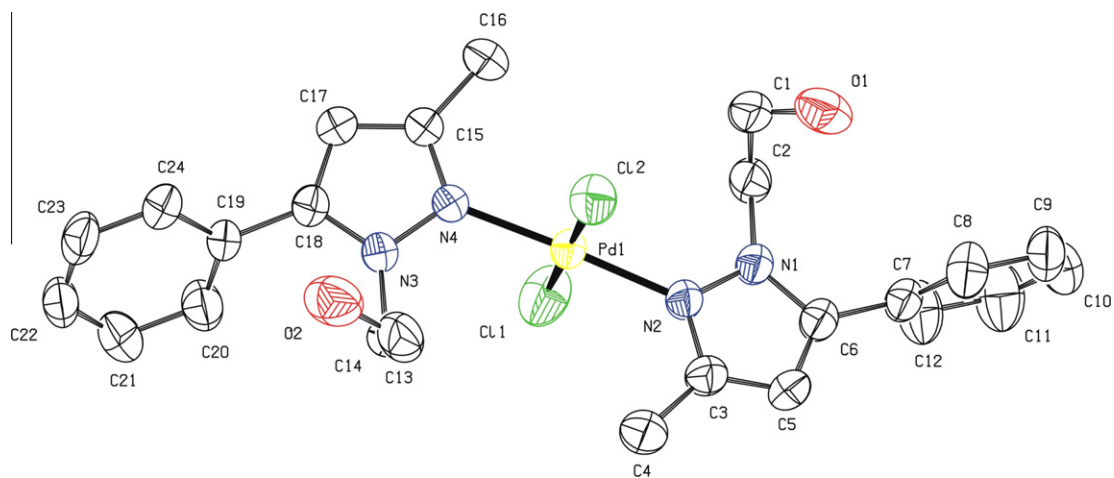


Fig. 5. ORTEP diagram of complex $[\text{PdCl}_2(\text{L2})_2]$ (**2**) showing an atom labelling scheme. 50% Amplitude displacement ellipsoids are shown. Hydrogen atoms are omitted for clarity.

Table 2
Selected bond lengths (Å) and bond angles (°) for $[\text{PdCl}_2(\text{L1})_2]$ (**1**) and $[\text{PdCl}_2(\text{L2})_2]$ (**2**).

1		2	
Pd–N(2)	1.992(5)	Pd–N(2)	2.010(5)
Pd–N(4)	1.998(5)	Pd–N(4)	2.007(5)
Pd–Cl(1)	2.279(2)	Pd–Cl(1)	2.274(2)
Pd–Cl(2)	2.282(2)	Pd–Cl(2)	2.318(2)
N(2)–Pd–N(4)	178.9(2)	N(2)–Pd–N(4)	177.2(2)
N(2)–Pd–Cl(1)	90.3(2)	N(2)–Pd–Cl(1)	89.4(1)
N(4)–Pd–Cl(1)	90.3(2)	N(4)–Pd–Cl(1)	88.6(1)
N(2)–Pd–Cl(2)	89.8(2)	N(2)–Pd–Cl(2)	90.4(1)
N(4)–Pd–Cl(2)	89.7(2)	N(4)–Pd–Cl(2)	91.7(1)
Cl(1)–Pd–Cl(2)	179.7(1)	Cl(1)–Pd–Cl(2)	179.1(1)

The crystal structures of **1** and **2**, consist of discrete Pd(II) molecules connected by hydrogen bonds. The Pd(II) is linked to two ligand molecules (**L1** or **L2**) via $\kappa^1\text{-N}_{\text{pz}}$ and finishes its coordination with two chlorine atoms in a *trans* disposition. The Pd(II) centre presents a typical square planar geometry (with a slight tetrahedral distortion) in which the largest deviation from the mean coordination plane is $-0.004(1)$ Å for **1**, and $0.006(1)$ Å for **2**. The palladium centre is approximately coplanar with the four coordinating atoms. The values of N–Pd–N and Cl–Pd–Cl angles are between $177.2(2)^\circ$ and $179.7(1)^\circ$. Moreover, the values of N–Pd–Cl angles are between $88.6(1)^\circ$ and $90.3(2)^\circ$. The *cis* angles N–Pd–Cl deviate from the ring angle in $\approx 1^\circ$, the deviation is the same order in the similar complexes [8].

In both complexes, ligands (**L1** and **L2**, respectively) are not planar. The phenyl groups twisted with respect to the pyrazole groups. The dihedral angles between ph and pz are $73.5(3)^\circ$ and $69.9(4)^\circ$ for **1**, and $84.2(4)^\circ$ and $58.6(3)^\circ$ for **2**. The ph–pz dihedral angles are in the interval described in the literature [5a,5c,9a,23]. The hydroxyethyl group, bonded to N_{pz} atom, moves away from the chelating plane giving a torsion angle N–C–O, $80.7(9)^\circ$ for **1** and $61.4(8)^\circ$ and $63.3(8)^\circ$ for **2**, respectively. These values are the same order than that found in other complexes described in the literature [5e,24]. However, it has to be remarked that in the complex **1** the hydroxyethyl group is disordered over two orientations with site-occupancy factors of 0.634(9) and 0.366(9).

The N1 and N3-hydroxyalkyl chains are in *anti* disposition with respect of the plane of coordination of metal. The X-ray powder diffraction pattern of **1** and **2** corroborate the presence of the unique *anti* conformer in the solid state. The $[PdCl_2(N_{pz})_2]$ core (containing terminal chlorine atoms) is found in 69 complexes described in the literature (39 of the complexes have *trans* geometry and thirty are *cis*) [6]. The values of distances Pd–N [1.992(5) Å, 1.998(5) Å; 2.007(5), 2.010(5) Å] and Pd–Cl [2.279(2) Å; 2.282(2) Å; 2.274(2) Å; 2.318(2) Å] are in agreement with the values described in the literature: Pd–N [1.989–2.042 Å] and Pd–Cl [2.280–2.349 Å] [6].

Nevertheless, the molecular packing and the intermolecular interactions in complexes **1** and **2** are very different. The crystal structure of complex **1** is tetragonal $I4_1/a$ with 16 Pd(II) molecules in the unit cell. Four molecules related by a 4-fold rotoinversion axis form a tetrameric building unit through hydrogen bonding between the hydroxyethyl hydrogen atom at O1 and the oxygen atom O2, symmetry code $\frac{3}{4} - y, \frac{3}{4} + x, \frac{3}{4} - z$. These tetrameric units are further connected by hydrogen bonding involving the hydroxyethyl hydrogen atom at O2 and the oxygen atom O1, symmetry code $-\frac{1}{2} + x, y, \frac{1}{2} - z$ (see Table 3). Description of the hydrogen bonds has been made with the position of the hydroxyethyl group with the highest site-occupancy factor. Additional C–H...Cl hydrogen interactions connect the four-units along the [001] direction (Table 3). Furthermore, some weak C–H... π interactions involving the phenyl and pyrazole rings, play a role in the stabilization of the crystal structure (see Table 4). These interactions and the cooperative effect form a 3D supramolecular network where the molecules are arranged in layers parallel to [001] direction and the phenyl rings are nearly perpendicular in successive layers (Fig. 6).

The crystal structure of complex **2** is triclinic $P\bar{1}$ with two Pd(II) molecules in the unit cell. The molecules are bonded by intermolecular hydrogen bonds between the hydroxyethyl hydrogen atom at O1 and the hydroxyethyl oxygen atom O2 of the translation related molecule (Table 5), forming chains that elongate in the direction of the *a*-axis (Fig. 7). These chains are connected by O–H...Cl hydrogen bonding between the hydroxyethyl hydrogen atom at O2 and the chlorine atom Cl2 of the inversion symmetry related molecule (Table 5). These intermolecular interactions can be considered as “moderate” on the basis of the contact distances and

Table 3
Geometrical parameters of hydrogen bonds in complex **1**.

D–H...A	D–H (Å)	D–H...A (Å)	D...A (Å)	D–H...A ($^\circ$)
O(1)–H(10)...O(2) ⁱ	0.82	1.92	2.75(2)	176
O(2)–H(20)...O(1) ⁱⁱ	0.82	2.42	3.21(2)	162
C(4)–H(4B)...Cl(1) ⁱⁱⁱ	0.96	2.73	3.643(9)	159
C(4)–H(4C)...Cl(1) ^{iv}	0.96	2.80	3.704(9)	157
C(16)–H(16B)...Cl(2) ^v	0.96	2.95	3.864(9)	160
C(23)–H(23)...Cl(2) ^{vi}	0.93	2.92	3.639(9)	135

Symmetry codes for complex **1**: (i) $\frac{3}{4} - y, \frac{3}{4} + x, \frac{3}{4} - z$; (ii) $-\frac{1}{2} + x, y, \frac{1}{2} - z$; (iii) $\frac{1}{4} - y, \frac{1}{4} + x, \frac{1}{4} - z$; (iv) $-\frac{1}{4} + y, \frac{3}{4} - x, -\frac{1}{4} + z$; (v) $-\frac{3}{4} + y, \frac{1}{4} - x, \frac{1}{4} + z$; (vi) $-\frac{3}{4} + y, \frac{3}{4} - x, \frac{3}{4} - z$.

Table 4
Geometrical parameters of C–H... π interactions in complex **1**.

C–H...Cg	H...Cg (Å)	D–H...Cg (Å)	D–H...A ($^\circ$)
C(1)–H(1A)...Cg(4) ⁱ	2.93	3.70(1)	138
C(9)–H(9)...Cg(2) ⁱⁱ	2.74	3.562(8)	149
C(11)–H(11)...Cg(1) ⁱⁱⁱ	2.80	3.635(8)	149
C(17)–H(17)...Cg(4) ^{iv}	2.92	3.821(7)	164
C(23)–H(23)...Cg(2) ^v	3.00	3.792(8)	144

Symmetry codes for complex **1**: (i) x, y, z ; (ii) $-\frac{3}{4} + y, \frac{1}{4} - x, \frac{1}{4} + z$; (iii) $\frac{1}{4} - y, \frac{1}{4} + x, \frac{1}{4} - z$; (iv) $-x, \frac{3}{2} - y, z$; (v) $\frac{3}{4} - y, \frac{3}{4} + x, \frac{3}{4} - z$. Cg(4), Cg(2) and Cg(1) are the centroids of the phenyl and pyrazole rings numbered C(7A)–C(12A), C(7)–C(12) and C(7B)–C(12B), respectively.

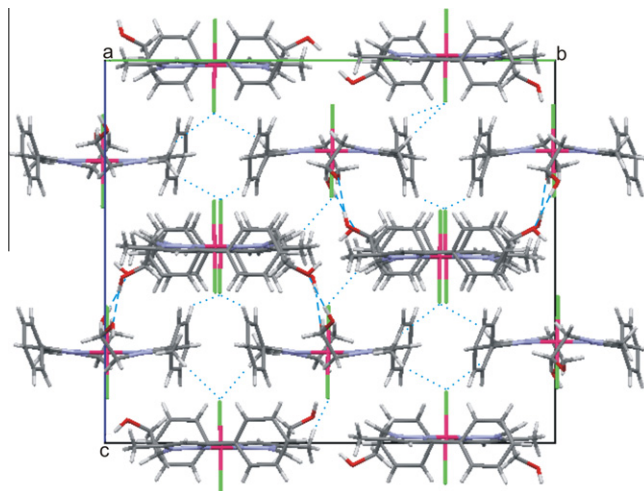


Fig. 6. Crystal packing of complex **1**, viewed along [100] direction. Dashed lines represent hydrogen bonds.

Table 5
Geometrical parameters of hydrogen bonds in complex **2**.

O–H...A	O–H (Å)	O–H...A (Å)	O...A (Å)	O–H...A ($^\circ$)
O(2)–H(20)...O(1) ⁱ	0.90(2)	1.90(2)	2.747(8)	156(2)
O(1)–H(10)...Cl(2) ⁱⁱ	0.82	2.50	3.276(6)	158

Symmetry codes for complex **2**: (i) $-1 + x, y, z$; (ii) $1 - x, -y, 2 - z$.

angles [25]. Furthermore the supramolecular structure is also stabilized by C–H... π interactions involving the phenyl rings. The C–H...Cg contact distances between the H atoms and the centroid of the neighbouring phenyl ring are: C(1)–H(1A)...Cg(4) 2.94 Å, symmetry code $1 + x, y, z$; C(4)–H(4C)...Cg(4) 2.92 Å, symmetry code $x, -1 + y, z$; Cg(4) is the centroid of the phenyl ring numbered C(19)–C(24).

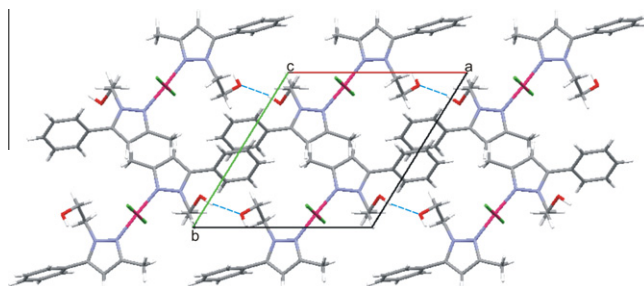


Fig. 7. Crystal packing of complex **2**, generated through hydrogen bonds and C–H... π interactions. Dashed lines represent hydrogen bonds.

3. Conclusions

The ligands **L1** and **L2** reacts with $[\text{MCl}_2(\text{CH}_3\text{CN})_2]$ ($\text{M} = \text{Pd}(\text{II}), \text{Pt}(\text{II})$) to give the *trans*- $[\text{MCl}_2\text{L}_2]$ ($\text{M} = \text{Pd}(\text{II}), \text{Pt}(\text{II}); \text{L} = \text{L1}, \text{L2}$) complexes. When $\text{M} = \text{Pd}(\text{II})$ and $\text{L} = \text{L1}$ (**1**), **L2** (**2**), the NMR study is consistent with a very slow rotation around Pd–N bond, so that two conformational isomers, *anti* and *syn*, can be observed in solution. The regioisomer ratio in solution is 1:0.8 (**1**) and 1:0.4 (**2**), *anti*:*syn*, respectively. The position of *N1*-substituting, hydroxyethyl chain is the responsible of the different intensity ratio observed for two species. In the solid state only the *anti* isomer is observed. A different behaviour is observed in the complexes *trans*- $[\text{PtCl}_2\text{L}_2]$ ($\text{L} = \text{L1}, \text{L2}$), which show only one signal for each type of proton and carbon. The species present in solution is the *anti* isomer. Several types of intermolecular interactions, specially hydrogen bonds but also C–H... π links, define the overall 3D supramolecular structure observed in the solid state.

4. Experimental

4.1. General methods

All reactions were performed under a nitrogen atmosphere using the usual vacuum line and Schlenk techniques. Solvents were dried and distilled by standard methods and deoxygenated in the vacuum line before being used. All reagents were commercial grade and were used without further purification. 1-Phenyl-1,3-butanedione, $[\text{PdCl}_2(\text{CH}_3\text{CN})_2]$ and $[\text{PtCl}_2(\text{CH}_3\text{CN})_2]$ were prepared as described in the literature [9,13,14].

Elemental analysis (C, N, H) and mass spectra (ESI⁺-MS) were carried out by the staff of the Chemical Analysis Services of the Universitat Autònoma de Barcelona on a Carlo Erba CHNS EA-1108 instrument and an Esquire 3000 ion trap mass spectrometer from Bruker Daltonics, respectively. Conductivity measurements were performed at room temperature in 10^{-3} M methanol solutions employing a CiberScan instrument CON 500 conductimeter. Infrared spectra were recorded on NaCl disks, as KBr pellets or polyethylene films in the range 4000 to 200 cm^{-1} under a nitrogen atmosphere employing a Perkin Elmer FT-2000 spectrophotometer. The ^1H and $^{13}\text{C}\{^1\text{H}\}$ NMR spectra and bidimensional NMR spectra were run on an NMR-FT Bruker AC-250 spectrometer. All NMR experiments were recorded on CDCl_3 solvent under nitrogen. ^1H and $^{13}\text{C}\{^1\text{H}\}$ NMR chemical shifts (δ) were determined relative to internal TMS and are given in ppm. The $^{195}\text{Pt}\{^1\text{H}\}$ NMR spectra were recorded at 298 K in CDCl_3 solutions, and 77 Mz on a DPX-360 MHz Bruker spectrometer using aqueous solutions of $[\text{PtCl}_6]^{2-}$ (0 ppm) as an external reference and delay times 0.01 s.

4.2. Synthesis of 2-(5-methyl-3-phenyl-1H-pyrazol-1-yl)ethanol (**L1**) and 2-(3-methyl-5-phenyl-1H-pyrazol-1-yl)ethanol (**L2**)

1-Phenyl-1,3-butanedione (1.2 mmol, 0.19 g) was dissolved in absolute ethanol (25 ml). To this solution 2-hydroxyethylhydrazine (1.3 mmol, 0.10 g) was added and the mixture was stirred at room temperature for 16 h. After removing the solvent under vacuum, the product was extracted from the oil residuum with $\text{H}_2\text{O}/\text{CHCl}_3$. The collected organic phases were dried with anhydrous calcium sulphate and removed under vacuum. Ligands were obtained in 98% yield as oils with sufficient purity (^1H NMR). The separation of regioisomers was done by silica column chromatography using ethyl acetate as eluent.

In the case of the synthesis at low temperature, the same procedure was followed. Reaction was performed during the same time but at -84°C using a cooling mixture of ethyl acetate/liquid N_2 .

4.2.1. Ligand **L1**

Yield: 57%. m.p = $20\text{--}25^\circ\text{C}$. Anal. Calc. for $\text{C}_{12}\text{H}_{14}\text{N}_2\text{O}$ (202.2): C, 71.26; H, 6.98; N, 13.85. Found: C, 71.41; H, 6.72; N, 13.83%. MS(ESI⁺): m/z (%) = 225 (41) $[\text{L1}+\text{Na}]^+$; 203 (100) $[\text{L1}+\text{H}]^+$. IR ($\text{NaCl}/\text{cm}^{-1}$): $\nu(\text{O-H})$ 3233, $\nu(\text{C-H})_{\text{ar}}$ 3040, $\nu(\text{C-H})_{\text{al}}$ 2929, 2855, $[\nu(\text{C=C}), \nu(\text{C=N})]_{\text{ph}}$ 1654, $[\nu(\text{C=C}), \nu(\text{C=N})]_{\text{pz}}$ 1604, $[\delta(\text{C=C}), \delta(\text{C=N})]$ 1457, $\delta(\text{C-H})_{\text{ip}}$ 1089, $\delta(\text{C-H})_{\text{oop}}$ 697. ^1H NMR (CDCl_3 solution, 250 MHz, 298 K) δ = 8.22–7.81 [m, 4H, H_{ph}], 7.76 [d, 1H, 3J 5.1 Hz, $H_{\text{orto ph}}$], 6.19 [s, 1H, $\text{CH}(\text{pz})$], 4.28 [t, 2H, 3J 5.3 Hz, $\text{NCH}_2\text{CH}_2\text{OH}$], 4.13 [br, 1H, $\text{NCH}_2\text{CH}_2\text{OH}$], 4.06 [t, 2H, 3J 5.3 Hz, $\text{NCH}_2\text{CH}_2\text{OH}$], 2.80 [s, 3H, CH_3]. $^{13}\text{C}\{^1\text{H}\}$ NMR (CDCl_3 solution, 63 MHz, 298 K) δ = 151.3 [C–ph], 140.3 [C– CH_3], 135.2 [C–Cph], 130.2–125.7 [Cph], 102.4 [CH(pz)], 61.5 [$\text{N}_{\text{pz}}\text{CH}_2\text{CH}_2\text{OH}$], 50.1 [$\text{N}_{\text{pz}}\text{CH}_2\text{CH}_2\text{OH}$], 11.9 [pz– CH_3].

4.2.2. Ligand **L2**

Yield: 32%. Anal. Calc. for $\text{C}_{12}\text{H}_{14}\text{N}_2\text{O}$ (202.2): C, 71.26; H, 6.98; N, 13.85. Found: C, 71.12; H, 6.85; N, 13.74%. MS(ESI⁺): m/z (%) = 225 (47) $[\text{L2}+\text{Na}]^+$; 203 (100) $[\text{L2}+\text{H}]^+$. IR ($\text{NaCl}/\text{cm}^{-1}$): $\nu(\text{O-H})$ 3235, $\nu(\text{C-H})_{\text{ar}}$ 3038, $\nu(\text{C-H})_{\text{al}}$ 2920, 2874, $[\nu(\text{C=C}), \nu(\text{C=N})]_{\text{ph}}$ 1672, $[\nu(\text{C=C}), \nu(\text{C=N})]_{\text{pz}}$ 1597, $[\delta(\text{C=C}), \delta(\text{C=N})]$ 1452, $\delta(\text{C-H})_{\text{ip}}$ 1083, $\delta(\text{C-H})_{\text{oop}}$ 782. ^1H NMR (CDCl_3 solution, 250 MHz, 298 K) δ = 8.04–7.51 [m, 4H, H_{ph}], 7.42 [d, 1H, 3J 4.7 Hz, $H_{\text{orto ph}}$], 5.96 [s, 1H, $\text{CH}(\text{pz})$], 4.16 [t, 2H, 3J 5.1 Hz, $\text{NCH}_2\text{CH}_2\text{OH}$], 3.95 [t, 2H, 3J 5.1 Hz, $\text{NCH}_2\text{CH}_2\text{OH}$], 3.91 [br, 1H, $\text{NCH}_2\text{CH}_2\text{OH}$], 2.32 [s, 3H, CH_3]. $^{13}\text{C}\{^1\text{H}\}$ NMR (CDCl_3 solution, 63 MHz, 298 K) δ = 152.4 [C–ph], 138.2 [C– CH_3], 131.7 [C–Cph], 129.4–122.6 [Cph], 105.6 [CH(pz)], 61.9 [$\text{N}_{\text{pz}}\text{CH}_2\text{CH}_2\text{OH}$], 50.5 [$\text{N}_{\text{pz}}\text{CH}_2\text{CH}_2\text{OH}$], 13.3 [pz– CH_3].

4.3. Synthesis of the complexes $[\text{PdCl}_2(\text{L1})_2]$ (**1**) and $[\text{PdCl}_2(\text{L2})_2]$ (**2**)

The appropriate ligand (**L1**, **L2**: 0.40 mmol, 0.081 g) dissolved in dry acetonitrile (25 ml) was added slowly to a solution of $[\text{PdCl}_2(-\text{CH}_3\text{CN})_2]$ (0.20 mmol, 0.052 g) in dry acetonitrile (50 ml). The resulting solution was cooled down to 0°C and diethyl ether was then added to induce precipitation. The orange solids were filtered off, washed twice with 10 ml of diethyl ether and dried under vacuum.

4.3.1. Complex **1**

Yield: 82%. $T = 213^\circ\text{C}$ decomp. Anal. Calc. for $\text{C}_{24}\text{H}_{28}\text{N}_4\text{O}_2\text{PdCl}_2$ (581.8): C, 49.60; H, 4.85; N, 9.63. Found: C, 49.37; H, 4.62; N, 9.32%. MS(ESI⁺): m/z (%) = 546 (100) $[\text{PdCl}(\text{L1})_2]^+$. Conductivity ($\Omega^{-1}\text{ cm}^2\text{ mol}^{-1}$, 1.08×10^{-3} M in methanol): 30. IR ($\text{KBr}/\text{cm}^{-1}$): $\nu(\text{O-H})$ 3309, $\nu(\text{C-H})_{\text{ar}}$ 3117, $\nu(\text{C-H})_{\text{al}}$ 2936, $[\nu(\text{C=C}), \nu(\text{C=N})]$ 1559, $[\delta(\text{C=C}), \delta(\text{C=N})]$ 1448, $\delta(\text{C-H})_{\text{ip}}$ 1040, $\delta(\text{C-H})_{\text{oop}}$ 768. (Polyethylene/ cm^{-1}): $\nu(\text{Pd-N})$ 487, $\nu(\text{Pd-Cl})$ 351. ^1H NMR (CDCl_3 solution, 250 MHz, 298 K) δ isomer *anti* 8.10 [d, 2H, 3J 7.4 Hz, $H_{\text{orto ph}}$], 7.60 [s, 8H, H_{ph}], 6.33 [s, 2H, $\text{CH}(\text{pz})$], 5.41 [t, 4H, 3J 6.6 Hz, $\text{NCH}_2\text{CH}_2\text{OH}$], 4.31 [t, 4H, 3J 6.6 Hz, $\text{NCH}_2\text{CH}_2\text{OH}$], 3.15 [br, 2H, $\text{NCH}_2\text{CH}_2\text{OH}$], 2.38 [s, 6H, CH_3]. δ isomer *syn* 7.89 [d, 2H, 3J 8.1 Hz, $H_{\text{orto ph}}$], 7.16 [s, 8H, H_{ph}], 6.31 [s, 2H, $\text{CH}(\text{pz})$], 4.78 [t, 4H, 3J 5.7 Hz, $\text{NCH}_2\text{CH}_2\text{OH}$], 4.01 [t, 4H, 3J 5.7 Hz, $\text{NCH}_2\text{CH}_2\text{OH}$], 3.14–2.84 [br, 2H, $\text{NCH}_2\text{CH}_2\text{OH}$], 2.35 [s, 6H, CH_3]. $^{13}\text{C}\{^1\text{H}\}$ NMR (CDCl_3 solution, 63 MHz, 298 K) δ isomer *anti* 149.2 [C–ph], 140.3 [C– CH_3], 133.8 [C–Cph], 129.8–128.5 [Cph], 108.1 [CH(pz)], 60.3 [$\text{N}_{\text{pz}}\text{CH}_2\text{CH}_2\text{OH}$], 51.4 [$\text{N}_{\text{pz}}\text{CH}_2\text{CH}_2\text{OH}$], 12.3 [pz– CH_3]. δ isomer *syn* 149.0 [C–ph], 139.9 [C– CH_3], 133.6 [C–Cph], 129.8–128.5 [Cph], 108.4 [CH(pz)], 60.1 [$\text{N}_{\text{pz}}\text{CH}_2\text{CH}_2\text{OH}$], 51.7 [$\text{N}_{\text{pz}}\text{CH}_2\text{CH}_2\text{OH}$], 12.6 [pz– CH_3].

4.3.2. Complex **2**

Yield: 75%. $T = 227^\circ\text{C}$ decomp. Anal. Calc. for $\text{C}_{24}\text{H}_{28}\text{N}_4\text{O}_2\text{PdCl}_2$ (581.8): C, 49.60; H, 4.85; N, 9.63. Found: C, 49.57; H, 4.65; N, 9.35%. MS(ESI⁺): m/z (%) = 546 (100) $[\text{PdCl}(\text{L2})_2]^+$. Conductivity

($\Omega^{-1} \text{ cm}^2 \text{ mol}^{-1}$, $1.15 \times 10^{-3} \text{ M}$ in methanol): 19. IR (KBr/ cm^{-1}): $\nu(\text{O-H})$ 3398, $\nu(\text{C-H})_{\text{ar}}$ 3045, $\nu(\text{C-H})_{\text{al}}$ 2938, [$\nu(\text{C}=\text{C})$, $\nu(\text{C}=\text{N})$] 1555, [$\delta(\text{C}=\text{C})$, $\delta(\text{C}=\text{N})$] 1500, $\delta(\text{C-H})_{\text{ip}}$ 1014, $\delta(\text{C-H})_{\text{oop}}$ 772. (Polyethylene/ cm^{-1}): $\nu(\text{Pd-N})$ 494, $\nu(\text{Pd-Cl})$ 355. ^1H NMR (CDCl_3 solution, 250 MHz, 298 K) δ isomer *anti* 7.47 [s, 10H, H_{ph}], 6.19 [s, 2H, $\text{CH}(\text{pz})$], 4.97 [t, 4H, 3J 6.4 Hz, $\text{NCH}_2\text{CH}_2\text{OH}$], 4.22 [t, 4H, 3J 6.4 Hz, $\text{NCH}_2\text{CH}_2\text{OH}$], 3.03 [s, 6H, CH_3], 2.62 [br, 2H, $\text{NCH}_2\text{CH}_2\text{OH}$]. δ isomer *syn* 7.35 [s, 10H, H_{ph}], 6.17 [s, 2H, $\text{CH}(\text{pz})$], 4.75 [t, 4H, 3J 5.8 Hz, $\text{NCH}_2\text{CH}_2\text{OH}$], 3.88 [t, 4H, 3J 5.8 Hz, $\text{NCH}_2\text{CH}_2\text{OH}$], 2.95 [s, 6H, CH_3], 2.64–2.62 [br, 2H, $\text{NCH}_2\text{CH}_2\text{OH}$]. $^{13}\text{C}\{^1\text{H}\}$ NMR (CDCl_3 solution, 63 MHz, 298 K) δ isomer *anti* 150.2 [C-ph], 141.7 [C- CH_3], 134.2 [C-Cph], 130.1–129.3 [Cph], 109.1 [CH(pz)], 62.0 [$\text{N}_{\text{pz}}\text{CH}_2\text{CH}_2\text{OH}$], 52.5 [$\text{N}_{\text{pz}}\text{CH}_2\text{CH}_2\text{OH}$], 15.7 [pz- CH_3]. δ isomer *syn* 149.8 [C-ph], 141.9 [C- CH_3], 133.8 [C-Cph], 130.1–129.3 [Cph], 108.9 [CH(pz)], 61.3 [$\text{N}_{\text{pz}}\text{CH}_2\text{CH}_2\text{OH}$], 52.2 [$\text{N}_{\text{pz}}\text{CH}_2\text{CH}_2\text{OH}$], 15.6 [pz- CH_3].

4.4. Synthesis of the complexes $[\text{PtCl}_2(\mathbf{L1})_2]$ (**3**) and $[\text{PtCl}_2(\mathbf{L2})_2]$ (**4**)

The appropriate ligand (**L1**, **L2**: 0.25 mmol, 0.051 g) dissolved in dry acetonitrile (25 ml) was added slowly to a solution of $[\text{PtCl}_2(\text{CH}_3\text{CN})_2]$ (0.13 mmol, 0.045 g) in dry acetonitrile (50 ml). The resulting solution was stirred and refluxed for 24 h and concentrated on a vacuum line to one fifth of the initial volume. The yellow solids were filtered off, washed twice with 5 ml of diethyl ether and dried under vacuum.

4.4.1. Complex **3**

Yield: 68%. $T = 236^\circ\text{C}$ decomp. *Anal.* Calc. for $\text{C}_{24}\text{H}_{28}\text{N}_4\text{O}_2\text{PtCl}_2$ (670.5): C, 43.05; H, 4.21; N, 8.36. Found: C, 42.81; H, 4.07; N, 8.43%. MS(ESI+): m/z (%) = 635 (100) $[\text{PtCl}(\mathbf{L1})_2]^+$. Conductivity ($\Omega^{-1} \text{ cm}^2 \text{ mol}^{-1}$, $1.09 \times 10^{-3} \text{ M}$ in methanol): 18. IR (KBr/ cm^{-1}): $\nu(\text{O-H})$ 3435, $\nu(\text{C-H})_{\text{ar}}$ 3028, $\nu(\text{C-H})_{\text{al}}$ 2968, 2931, [$\nu(\text{C}=\text{C})$, $\nu(\text{C}=\text{N})$] 1554, [$\delta(\text{C}=\text{C})$, $\delta(\text{C}=\text{N})$] 1437, $\delta(\text{C-H})_{\text{ip}}$ 1032, $\delta(\text{C-H})_{\text{oop}}$ 812. (Polyethylene/ cm^{-1}): $\nu(\text{Pt-N})$ 458, $\nu(\text{Pt-Cl})$ 344. ^1H NMR (CDCl_3 solution, 250 MHz, 298 K) δ isomer *anti* 7.21 [s, 10H, H_{ph}], 6.03 [s, 2H, $\text{CH}(\text{pz})$], 4.91, [t, 4H, 3J 5.9 Hz, $\text{NCH}_2\text{CH}_2\text{OH}$], 3.96 [t,

4H, 3J 5.7 Hz, $\text{NCH}_2\text{CH}_2\text{OH}$], 2.84 [s, 6H, CH_3]. $^{13}\text{C}\{^1\text{H}\}$ NMR (CDCl_3 solution, 63 MHz, 298 K) δ isomer *anti* 153.1 [C-ph], 143.5 [C- CH_3], 137.2 [C-Cph], 131.4–128.7 [Cph], 108.9 [CH(pz)], 62.4 [$\text{N}_{\text{pz}}\text{CH}_2\text{CH}_2\text{OH}$], 52.7 [$\text{N}_{\text{pz}}\text{CH}_2\text{CH}_2\text{OH}$], 15.9 [pz- CH_3]. $^{195}\text{Pt}\{^1\text{H}\}$ NMR (CDCl_3 solution, 77 MHz, 298 K) δ isomer *anti* –2189 ppm.

4.4.2. Complex **4**

Yield: 62%. $T = 248^\circ\text{C}$ decomp. *Anal.* Calc. for $\text{C}_{24}\text{H}_{28}\text{N}_4\text{O}_2\text{PtCl}_2$ (670.5): C, 43.05; H, 4.21; N, 8.36. Found: C, 42.88; H, 4.32; N, 8.39%. MS(ESI+): m/z (%) = 635 (100) $[\text{PtCl}(\mathbf{L1})_2]^+$. Conductivity ($\Omega^{-1} \text{ cm}^2 \text{ mol}^{-1}$, $9.20 \times 10^{-4} \text{ M}$ in methanol): 26. IR (KBr/ cm^{-1}): $\nu(\text{O-H})$ 3448, $\nu(\text{C-H})_{\text{ar}}$ 3052, $\nu(\text{C-H})_{\text{al}}$ 2970, 2919, [$\nu(\text{C}=\text{C})$, $\nu(\text{C}=\text{N})$] 1559, [$\delta(\text{C}=\text{C})$, $\delta(\text{C}=\text{N})$] 1449, $\delta(\text{C-H})_{\text{ip}}$ 1029, $\delta(\text{C-H})_{\text{oop}}$ 803. (Polyethylene/ cm^{-1}): $\nu(\text{Pt-N})$ 462, $\nu(\text{Pt-Cl})$ 348. ^1H NMR (CDCl_3 solution, 250 MHz, 298 K) δ isomer *anti* 7.58 [s, 10H, H_{ph}], 6.14 [s, 2H, $\text{CH}(\text{pz})$], 5.41 [t, 4H, 3J 6.6 Hz, $\text{NCH}_2\text{CH}_2\text{OH}$], 4.02 [t, 4H, 3J 6.3 Hz, $\text{NCH}_2\text{CH}_2\text{OH}$], 2.35 [s, 6H, CH_3]. $^{13}\text{C}\{^1\text{H}\}$ NMR (CDCl_3 solution, 63 MHz, 298 K) δ isomer *anti* 152.4 [C-ph], 142.7 [C- CH_3], 135.6 [C-Cph], 129.8–128.5 [Cph], 108.0 [CH(pz)], 60.2 [$\text{N}_{\text{pz}}\text{CH}_2\text{CH}_2\text{OH}$], 51.4 [$\text{N}_{\text{pz}}\text{CH}_2\text{CH}_2\text{OH}$], 12.3 [pz- CH_3]. $^{195}\text{Pt}\{^1\text{H}\}$ NMR (CDCl_3 solution, 77 MHz, 298 K) δ isomer *anti* –2152 ppm.

4.5. X-ray crystal structures for compounds **L2** ligand, *trans*- $[\text{PdCl}_2(\mathbf{L1})_2]$ (**1**) and *trans*- $[\text{PdCl}_2(\mathbf{L2})_2]$ (**2**)

Suitable crystals for X-ray diffraction of **L2** ligand were obtained through crystallisation from ethyl acetate solution, and for compounds, *trans*- $[\text{PdCl}_2(\mathbf{L1})_2]$ (**1**) and *trans*- $[\text{PdCl}_2(\mathbf{L2})_2]$ (**2**) were obtained through crystallisation from a chloroform solution.

For compounds **L2**, **1** and **2**, a prismatic crystal was selected and mounted on a MAR345 diffractometer, with an image plate detector for **L2** and **1**, and on an Enraf-Nonius CAD4, four-circle diffractometer for **2**.

For **L2**, unit-cell parameters were determined from 456 reflections ($3^\circ < \theta < 31^\circ$) and refined by least-squares method. Intensities were collected with graphite monochromatized Mo $K\alpha$ radiation.

Table 6
Crystallographic data for **L2**, **1** and **2**.

	L2	1	2
Formula	$\text{C}_{12}\text{H}_{14}\text{N}_2\text{O}$	$\text{C}_{24}\text{H}_{28}\text{Cl}_2\text{N}_4\text{O}_2\text{Pd}$	$\text{C}_{24}\text{H}_{28}\text{Cl}_2\text{N}_4\text{O}_2\text{Pd}$
Molecular weight	202.25	581.80	581.80
T (K)	293(2)	293(2)	293(2)
Crystal System	triclinic	tetragonal	triclinic
Space group	$P\bar{3}m1$	$I4_1/a$	$P\bar{3}m1$
<i>Unit cell dimensions</i>			
a (Å)	10.289(7)	22.7902(12)	11.100(6)
b (Å)	11.777(9)	22.7902(12)	11.611(3)
c (Å)	20.067(4)	19.2949(7)	12.210(4)
α (°)	86.11(3)	90	106.82(3)
β (°)	89.46(2)	90	100.06(4)
γ (°)	64.57(2)	90	116.36(4)
Z	8	16	2
V (Å ³)	2190(2)	10021.6(8)	1262.6(12)
D_{calc} (g cm ⁻³)	1.227	1.542	1.530
μ (mm ⁻¹)	0.080	0.982	0.975
$F(000)$	864	4736	592
Crystal size (mm)	$0.19 \times 0.18 \times 0.17$	$0.2 \times 0.1 \times 0.1$	$0.09 \times 0.08 \times 0.07$
θ range (°)	1.92–25.03	1.38–24.92	2.12–29.97
Index range	$-11 \leq h \leq 12$, $-11 \leq k \leq 11$, $0 \leq l \leq 23$	$-19 \leq h \leq 18$, $0 \leq k \leq 27$, $0 \leq l \leq 22$	$-15 \leq h \leq 15$, $-16 \leq k \leq 15$, $0 \leq l \leq 17$
Reflections collected/unique	8145/5034 [$R_{\text{int}} = 0.0352$]	27967/4372 [$R_{\text{int}} = 0.0518$]	7327/7276 [$R_{\text{int}} = 0.0209$]
Completeness to θ (%)	65.3	85.5	100.0
Absorption correction	empirical	empirical	none
Maximum and minimum transmissions	0.99 and 0.98	0.91 and 0.89	–
Data/restraints/parameters	5034/8/542	3756/2/305	7326/3/303
Goodness-of-fit	1.050	1.151	1.009
Final R_1 , ωR_2	0.0468, 0.1447	0.0537, 0.1309	0.0644, 0.1329
R_1 (all data), ωR_2	0.0720, 0.1518	0.0816, 0.1470	0.1595, 0.1589
Largest difference in peak and hole (e Å ⁻³)	0.127 and –0.155	0.428 and –0.846	1.255 and –0.462

8145 reflections were measured in the range $1.92^\circ \leq \theta \leq 25.03^\circ$. 5034 of which were non-equivalent by symmetry ($R_{\text{int}}(\text{on } I) = 0.035$). 3092 reflections were assumed as observed applying the conditions $I > 2\sigma(I)$.

For **1**, unit-cell parameters were determined from automatic centring of 221 reflections ($3^\circ < \theta < 31^\circ$) and refined by least-squares method. Intensities were collected with graphite monochromatized Mo K α radiation. 27967 reflections were measured in the range $1.38^\circ \leq \theta \leq 24.92^\circ$. 4372 of which were non-equivalent by symmetry ($R_{\text{int}}(\text{on } I) = 0.051$). 3740 reflections were assumed as observed applying the conditions $I > 2\sigma(I)$.

For **2**, unit-cell parameters were determined from automatic centring of 25 reflections ($12^\circ < \theta < 21^\circ$) and refined by least-squares method. Intensities were collected with graphite monochromatized Mo K α radiation, using $\omega/2\theta$ scan-technique. 7327 reflections were measured in the range $2.12^\circ \leq \theta \leq 29.97^\circ$. 7276 of which were non-equivalent by symmetry ($R_{\text{int}}(\text{on } I) = 0.020$). 3801 reflections were assumed as observed applying the condition $I > 2\sigma(I)$. Three reflections were measured every two hours as orientation and intensity control, significant intensity decay was not observed.

For **L2**, **1** and **2**, Lorentz-polarisation but no absorption corrections were made.

All structures were solved by Direct methods, using SHELXS computer program (SHELXS-97) [26] and refined by full matrix least-squares method with SHELXL-97 [27] computer program using 8145 reflections for **L2**, 298 reflections for **1** and 7327 reflections for **2** (very negative intensities were not assumed).

For **L2**, the function minimised was $\Sigma w||F_o|^2 - |F_c|^2|^2$, where $w = [\sigma^2(I) + (0.0899P)^2]^{-1}$, and $P = (|F_o|^2 + 2|F_c|^2)/3$. For **1**, the function minimised was $\Sigma w||F_o|^2 - |F_c|^2|^2$, where $w = [\sigma^2(I) + (0.1011)P^2 + 36.974P]^{-1}$, and $P = (|F_o|^2 + 2|F_c|^2)/3$. For **2**, the function minimised was $\Sigma w||F_o|^2 - |F_c|^2|^2$, where $w = [\sigma^2(I) + (0.0083P)^2]^{-1}$ and $P = (|F_o|^2 + 2|F_c|^2)/3$.

For **L2**, **1** and **2**, all hydrogen atoms are computed and refined, using a riding model, with an isotropic temperature factor equal to 1.2 times the equivalent temperature factor of the atom which is linked. The final $R(F)$ factor and $R_w(F^2)$ values as well as the number of parameters refined and other details concerning the refinement of the crystal structures are gathered in Table 6.

Acknowledgement

Support by the Spanish Ministerio de Educación y Cultura (Projects CTQ-2007-63913BQU and MAT2011-27225) gratefully acknowledged.

Appendix A. Supplementary material

CCDC 872758, 872759 and 872760 contain the supplementary crystallographic data for compounds **L2**, **1** and **2**, respectively. These data can be obtained free of charge from The Cambridge Crystallographic Data Centre via www.ccdc.cam.ac.uk/data_request/cif.

References

- [1] (a) J.J. Li, G.W. Gribble, Palladium in Heterocyclic Chemistry, Pergamon, New York, USA, 2000; (b) J. Chakraborty, M.K. Saha, P. Benerjee, Inorg. Chem. Commun. 10 (2007) 671; (c) R.Y. Mawo, D.M. Johnson, J.L. Wood, I.P. Smoliakova, J. Organomet. Chem. 693 (2008) 33; (d) I. Ara, J. Forniés, R. Lasheras, A. Martín, V. Sicilia, Eur. J. Inorg. Chem. (2006) 948; (e) Y. Han, H.V. Huynh, G.K. Tan, Organometallics 26 (2007) 6581; (f) F. Niedermair, K. Waich, S. Kappaun, T. Mayr, G. Trimmel, K. Mereiter, C. Slugovc, Inorg. Chim. Acta 360 (2007) 2767;
- (g) C.-K. Koo, Y.-M. Ho, C.-F. Chow, M.H.-W. Lam, T.-C. Lau, W.-Y. Wong, Inorg. Chem. 46 (2007) 3603; (h) C.-K. Koo, B. Lam, S.-K. Leung, M.H.-W. Lam, W.-Y. Wong, J. Am. Chem. Soc. 128 (2006) 16434; (i) A.S. Lokin, W.J. Marshall, Y. Wang, Organometallics 24 (2005) 619.
- [2] (a) J. Pons, J. Ros, M. Llagostera, J.A. Pérez, M. Ferrer, Spanish Patent No. 01494, 2003.; (b) R.W.-Y. Sun, D.L. Ma, E.L.-M. Wong, C.M. Che, Dalton (2007) 4883; (c) A. Satake, T. Nakata, J. Am. Chem. Soc. 120 (1998) 10391; (d) C. Navarro-Ranninger, L. López-Solera, V.M. González, J.M. Pérez, A. Alvarez-Valdes, A. Martín, P.R. Raithby, J.R. Massaguer, C. Alonso, Inorg. Chem. 35 (1996) 5181; (e) C. Navarro-Ranninger, L. López-Solera, J.M. Pérez, J.R. Massaguer, C. Alonso, Appl. Organomet. Chem. 7 (1993) 57; (f) J.D. Higgins, L. Neely, S. Fricker, J. Inorg. Biochem. 49 (1993) 149.
- [3] (a) M. Guerrero, J. Pons, V. Branchadell, T. Parella, X. Solans, M. Font-Bardía, J. Ros, Inorg. Chem. 47 (2008) 11084; (b) J.M. Lehn, Science 260 (1993) 1762; (c) C.A. Mirkin, M.A. Ratner, Annu. Rev. Phys. Chem. 43 (1992) 719; (d) C. López, A. Caubet, S. Pérez, X. Solans, M. Font-Bardía, J. Organomet. Chem. 681 (2003) 82.
- [4] (a) V. Montoya, J. Pons, J. García-Antón, X. Solans, M. Font-Bardía, J. Ros, Organometallics 26 (2007) 3183; (b) M. Guerrero, J. Pons, J. Ros, J. Organomet. Chem. 695 (2010) 1957; (c) J. Dupont, M. Pfeffer, J. Spencer, Eur. J. Inorg. Chem. (2001) 1917; (d) D. Zim, A.S. Gruber, G. Ebeling, J. Dupont, A.L. Monteiro, Org. Lett. 2 (2000) 2881.
- [5] (a) V. Montoya, J. Pons, X. Solans, M. Font-Bardía, J. Ros, Inorg. Chim. Acta 358 (2005) 2312; (b) A. Boixassa, J. Pons, X. Solans, M. Font-Bardía, J. Ros, Inorg. Chim. Acta 357 (2004) 733; (c) A. Boixassa, J. Pons, X. Solans, M. Font-Bardía, J. Ros, Inorg. Chim. Acta 346 (2003) 151; (d) A. Boixassa, J. Pons, A. Virgili, X. Solans, M. Font-Bardía, J. Ros, Inorg. Chim. Acta 340 (2002) 49; (e) C. Luque, J. Pons, T. Calvet, M. Font-Bardía, J. García-Antón, J. Ros, Inorg. Chim. Acta 367 (2011) 35.
- [6] (a) Cambridge Structural Database, version 5.33, Cambridge Crystal Data Centre, Cambridge, UK, 2012.; (b) F.A. Allen, Acta Crystallogr., Sect. B 58 (2002) 380.
- [7] (a) G. Aragay, J. Pons, V. Branchadell, J. García-Antón, X. Solans, M. Font-Bardía, J. Ros, Aust. J. Chem. 63 (2010) 257; (b) M. Guerrero, J. Pons, T. Parells, M. Font-Bardía, T. Calvet, J. Ros, Inorg. Chem. 48 (2009) 8736; (c) A. Boixassa, J. Pons, X. Solans, M. Font-Bardía, J. Ros, Inorg. Chim. Acta 355 (2003) 254.
- [8] (a) T. Ying, W. Bao, Y. Zhang, W. Xu, Tetrahedron Lett. 37 (1996) 3885; (b) J. Tsuji, H. Nagashima, K. Hori, Chem. Lett. (1980) 257; (c) B.M. Perfetti, R. Levine, J. Am. Chem. Soc. 75 (1953) 626; (d) F.W. Swamer, C.R. Hauser, J. Am. Chem. Soc. 72 (1950) 1352.
- [9] (a) A. Chadghan, J. Pons, A. Caubet, J. Casabó, J. Ros, A. Alvarez-Larena, J.F. Piniella, Polyhedron 19 (2000) 855; (b) J. Pons, X. López, E. Benet, J. Casabó, F. Teixidor, F.J. Sánchez, Polyhedron 9 (1990) 2839; (c) J. Casabó, J. Pons, K.S. Siddiqi, F. Teixidor, E. Molins, C. Miravittles, J. Chem. Soc., Dalton Trans. (1989) 1401.
- [10] V. Montoya, J. Pons, J. García-Antón, X. Solans, M. Font-Bardía, J. Ros, Organometallics 26 (2007) 3183.
- [11] (a) D.H. Williams, I. Fleming, Spectroscopic Methods in Organic Chemistry, McGraw Hill, London, UK, 1995; (b) E. Pretch, T. Clerc, J. Seibl, W. Simon, Tables of Determination of Organic Compounds. ^{13}C NMR, ^1H NMR, IR, MS, UV/Vis, Chemical Laboratory Practice, Springer, Berlin, Germany, 1989.
- [12] S. Muñoz, J. Pons, J. Ros, M. Font-Bardía, C.A. Kilner, M.A. Halcrow, Inorg. Chim. Acta 373 (2011) 211.
- [13] S. Komiya, Synthesis of Organometallic Compounds: A Practice Guide, John Wiley & Sons, New York, USA, 1997.
- [14] F.P. Fanizi, F.P. Intini, L. Maresca, G. Natile, J. Chem. Soc., Dalton Trans. (1990) 199.
- [15] (a) L.K. Thompson, F.L. Lee, E.J. Gabe, Inorg. Chem. 27 (1988) 39; (b) W.J. Geary, Coord. Chem. Rev. 7 (1971) 81.
- [16] (a) A.R. Katritzky, C.W. Rens, Comprehensive Heterocyclic Chemistry: The Structure, Reactions, Synthesis, Uses of Heterocyclic Compounds, Pergamon Press, Oxford, UK, 1984; (b) D. Carmona, L.A. Oro, M.P. Lamala, J. Elguero, M.C. Apréda, C. Foces-Foces, F.H. Cano, Angew. Chem., Int. Ed. Engl. 25 (1986) 1114.
- [17] K. Nakamoto, Infrared and Raman Spectra of Inorganic and Coordination Compounds, fifth ed., Wiley & Sons, New York, USA, 1986.
- [18] J.A. Casares, P. Espinet, J.M. Martínez-Illarduya, Y.S. Lin, Organometallics 16 (1997) 770.
- [19] P.J. Stang, B. Olenyuk, A.M. Arif, Organometallics 14 (1995) 5281.
- [20] M. Fuss, H.U. Siehl, B. Olenyuk, P.J. Stang, Organometallics 18 (1999) 758.
- [21] M. Samiran, R. Mukherjee, J. Chem. Soc., Dalton Trans. (1992) 2337.
- [22] (a) M.C. Castellano, J. Pons, J. García-Antón, X. Solans, M. Font-Bardía, J. Ros, Inorg. Chim. Acta 361 (2008) 2491; (b) L. Scuzová, Z. Trávnicek, M. Zatloukal, I. Popa, Bioorg. Med. Chem. 14 (2006)

- 479;
- (c) I. Lakomska, E. Szlyk, J. Sitkowski, L. Kozerski, J. Wietrzyk, M. Pelczynska, A. Nasulewicz, A. Opolski, *J. Inorg. Biochem.* 98 (2004) 167;
- (d) Z. Trávníček, M. Maloň, M. Zatloukal, K. Dolezal, K. Strnad, J. Marek, *J. Inorg. Biochem.* 94 (2003) 307;
- (e) P. Tsiveriotis, N. Hadjiliadis, G. Slauropoulos, *Inorg. Chim. Acta* 261 (1997) 83;
- (f) Ch. Tessier, F.D. Rochon, *Inorg. Chim. Acta* 295 (1999) 25;
- (g) P.S. Pregosin, *Coord. Chem. Rev.* 33 (1982) 247.
- [23] (a) V. Montoya, J. Pons, X. Solans, M. Font-Bardía, J. Ros, *Inorg. Chim. Acta* 359 (2006) 25;
- (b) J.A. Pérez, J. Pons, X. Solans, M. Font-Bardía, J. Ros, *Inorg. Chim. Acta* 358 (2005) 617;
- (c) J. Pons, A. Chadghan, A. Alvarez-Larena, J.F. Piniella, J. Ros, *Inorg. Chim. Acta* 324 (2001) 342;
- (d) J. Pons, A. Chadghan, J. Casabó, A. Alvarez-Larena, J.F. Piniella, J. Ros, *Polyhedron* 20 (2001) 2531;
- (e) J. Pons, A. Chadghan, J. Casabó, A. Alvarez-Larena, J.F. Piniella, X. Solans, M. Font-Bardía, J. Ros, *Polyhedron* 20 (2001) 1029;
- (f) J. Pons, A. Chadghan, A. Alvarez-Larena, J.F. Piniella, J. Ros, *Inorg. Chem. Commun.* 4 (2001) 610;
- (g) J. Pons, A. Chadghan, J. Casabó, A. Alvarez-Larena, J.F. Piniella, J. Ros, *Inorg. Chem. Commun.* 3 (2000) 296.
- [24] V. Montoya, J. Pons, X. Solans, M. Font-Bardía, J. Ros, *Inorg. Chim. Acta* 360 (2007) 625.
- [25] T. Steiner, *Angew. Chem., Int. Ed.* 41 (2002) 48.
- [26] G.M. Sheldrick, *SHELXS 97*. Program for Crystal Structure Determination, University of Göttingen, Germany, 1997.
- [27] G.M. Sheldrick, *SHELXL 97*. Program for Crystal Structure Refinement, University of Göttingen, Germany, 1997.